01 Sep 1975

Structure of the Viscous Sublayer in Drag Reducing Channel Flows

W. G. Tiederman

A. J. Smith

D. K. Oldaker

STRUCTURE OF THE VISCOUS SUBLAYER IN DRAG-REDUCING CHANNEL FLOWS

W. G. Tiederman, A. J. Smith*, and D. K. Oldaker

School of Mechanical & Aerospace Engineering

Oklahoma State University

Stillwater, Oklahoma 74074

ABSTRACT

The objective of this study was to experimentally determine the effect of dilute, long-chain, polymer solutions upon the flow processes in a fully developed, two-dimensional turbulent channel flow. This was accomplished by making motion pictures of dye seeped through a slot into the viscous sublayer. The motion pictures were analyzed to determine the spanwise spacing and the bursting rate of the low-speed streaks that are characteristic of the sublayer structure.

INTRODUCTION

Numerous studies in Newtonian flows have shown that the two flow processes which are the most important in the production of turbulent kinetic energy are "sweeps" of high momentum fluid into the near-wall region and "bursts" of low momentum fluid from the "low-speed streaks" in the viscous sublayer. While these processes have been extensively studied in Newtonian flows, there have been few studies of the flow structure in drag-reducing flows. Those that are particularly relevant to this study are the streak-spacing study of Eckelman, Fortuna and Hanratty (1972) and the streak-spacing, bursting rate studies of Achia and Thompson (1974) and Donohue, Tiederman and Reischman (1972).

These three previous studies have each shown that the non-dimensional spanwise spacing of the low-speed streaks increases as the amount of drag reduction increases. While all three investigations yielded the same non-dimensional spacings for flows with less than 35% drag reduction, the three sets of results diverged as the amount of drag reduction increased. Therefore the initial objective of this study was to conduct streak-spacing experiments that would yield an explanation for these differences at the higher levels of drag reduction.

Oldaker (1974) conducted the bulk of these streak-spacing experiments with Separan AP 273. However, several experiments were also conducted with Magnifloc 837-A and Polyox WSR-301. Replicate experiments have also now been conducted. However, the new results that explain the previously reported differences are primarily due to the development of a new dye-slot visualization technique. This new technique uses fluorescent dye and side lighting to make visible very dilute concentrations of dye.

During these streak-spacing experiments in drag reducing flows, it was noted that some streaks were so long that they did not "burst" within the 3/4 m distance between the upstream dye slot and the end of the channel. This observation raised questions about the validity of previous bursting-rate measurements in drag-reducing flows because they were obtained with a technique which is based on the postulate that the observer will count the bursts from all of the streaks marked at or near an injection slot. Therefore the second objective was to critically examine bursting rate measurement techniques based upon wall-slot injection. In addition to experimentally testing this previously used technique, Smith (1975) introduced a new method which is based upon the postulate that it is possible to mark all of the bursting

*Present address: Mechanical-Nuclear Group, Brown and Root, Inc., Houston, TX

events within some region downstream of the dye slot. Smith's results in both water and drag-reducing flows will be compared with those of Achia and Thompson (1974), Donohue et al. (1972), Lu and Willmarth (1973), Laufer and Badri Narayanan (1971), Rao et al. (1971), and Offen and Kline (1974) in an attempt to identify how bursting rate measurements should be made with a dye slot technique and to determine how bursting rates are affected during drag reduction.

The major results and supporting data from the streak-spacing experiments will be presented. However, in this paper, the major emphasis will be placed upon the bursting rate measurements.

EXPERIMENTAL APPARATUS AND PROCEDURES

The experiments were conducted in the two-dimensional channel previously used by Donohue et al. (1972). The channel is 2.54 m long and 38.1 mm wide with an aspect ratio of 11.9. There are two spanwise dye slots located 44 and 51 channel widths downstream of the entrance. They are 178 mm long and 0.127 mm wide. The visualization took place in a region bounded by the upstream dye slot and the channel exit.

All of the flow visualization experiments were made by pressurizing a 13.63 m^3 upstream storage tank to force fluid through the channel and then to a drain. The large upstream tank was an important feature of the facility because it made it possible to conduct experiments for as long as 30 to 45 minutes in a "blow-down" mode of operation. Consequently, photographs of the flow processes were clear because dyed fluid was not recirculated and the homogeneous polymer solutions used in the drag reduction experiments were subjected to minimal mechanical degradation.

The wall shear, τ_w, and wall-shear velocity, u_τ, used in the data analysis were calculated from measurements of the pressure difference between two 3.18 mm diameter static wall taps located 457 mm apart. The upstream tap is 46.8 channel widths downstream of the entrance while the downstream tap is about 8 channel widths upstream of the channel's exit. A micromanometer with carbontetrachloride as the manometer fluid was used to measure the pressure difference. Mass-average velocities were calculated from flow rates that were obtained at each experimental condition by timing the collection of a measured volume of fluid.

The percentage drag reduction was defined to be

$$D_R = 100 \times (1 - \Delta P_p / \Delta P_s) \qquad (1)$$

Here ΔP_p is the pressure drop at the experimental flow rate of dilute polymer solution and ΔP_s is the pressure drop of water flowing at the same rate and temperature.

Flow Visualization

One of the most important experimental variables for both the streak-spacing and bursting rate measurements was the injection rate of the dye. For this reason the injection rates were carefully controlled and measured with a series of three Matheson rotameters. The temperature and polymer concentration of the injected dye solution was the same as that of the fluid flowing in the channel. Therefore, the rotameters were calibrated for each dye solution.

In the presentation of the data the ratio of the flow rate in the undisturbed viscous sublayer above the dye slot will be compared to the dye flow rate through the slot. This ratio, denoted as M, is a measure of dye used to mark the near-wall region. For these purposes, the non-dimensional thickness of the viscous sublayer was assumed to be $y^+ = 8$ for both the water and drag reducing flows. This assumption was based upon the measurements of Reischman and Tiederman (1975) which did not show any increase in the non-dimensional thickness of the viscous sublayer in drag-reducing flows. Therefore the operational definition of M is

$$M = \frac{d_{s_o} \int^{8\nu/u_\tau} U dy}{\dot{Q}_d} = \frac{32\, d_s\, \nu}{\dot{Q}_d} \qquad (2)$$

Here d_s is the length of dye slot being used and $\dot{Q}_d$ is the flow rate of the dye.

Streak Spacing. The lighting and viewing arrangement for the new fluorescent dye scheme used in the majority of the streak-spacing experiments are shown in Figure 1a. They differ from those of the technique used previously by Runstadler et al. (1963) and Donohue et al. (1972) in several ways. The most

important is that in the new technique the light enters from the top of the channel and the camera views the dye through the side wall of the channel. With this 90° orientation of the light source and viewer, and with a 0.12% solution of Rhodamine B dye, the near-wall flow structure appears to be self-illuminating. Moreover, the near-wall flow structure has a varying thickness and the side-lighting accentuates this feature by high-lighting one side of each bulge in the dye while the other side is in a shadow. The result is a three-dimensional picture of the near-wall region marked by the dye. Another important feature is that the fluorescent dye technique allows an observer to see much lower dye concentrations than the previously used back-lighting technique which naturally "washes out" the regions of low dye concentration. This feature allowed us to vary systematically the dye flow rate over a wide range as well as to see more details of the flow structure.

Most of the streak-spacing movies were taken with a Super 8 mm Beaulieu camera equipped with a f1.8, 25 mm lens. The filming speed was generally 24 to 36 frames per second. The films were viewed at 16 frames per second and then stopped at equal intervals of times for analysis.

Bursting Rate. The lighting and viewing arrangement for the bursting rate experiments shown in Figure 1b again used the brilliant orange color of fluorescing Rhodamine B dye to achieve good contrast in the motion pictures. The flow was viewed through the top of the channel by means of a single front surface mirror. The mirror box was 0.6 m long so that most of the region between the upstream dye slot and the end of the channel could be viewed by simply moving the lights and camera.

Most of the bursting rate movies were taken with black and white 4X reversal film and a 16 mm H-16 Bolex camera. A 75 mm f1.9 or a 75 mm f1.4 lens were used. The movies were analyzed frame by frame with a Bell and Howell time and motion projector.

Data Reduction

Streak Spacing. The basic scheme for deducing an average spanwise streak spacing was to count the number of streaks on a sufficient number of statistically independent frames of the motion pictures and then to calculate the average spanwise spacing, $\bar{\lambda}$, from

$$\bar{\lambda} = \frac{d_s}{N_s} \tag{3}$$

N_s is the average number of streaks per frame.

A streak was defined to be a clearly identifiable, single longitudinal structure which has a streamwise length of at least four times the apparent average spanwise spacing. There was no constraint placed

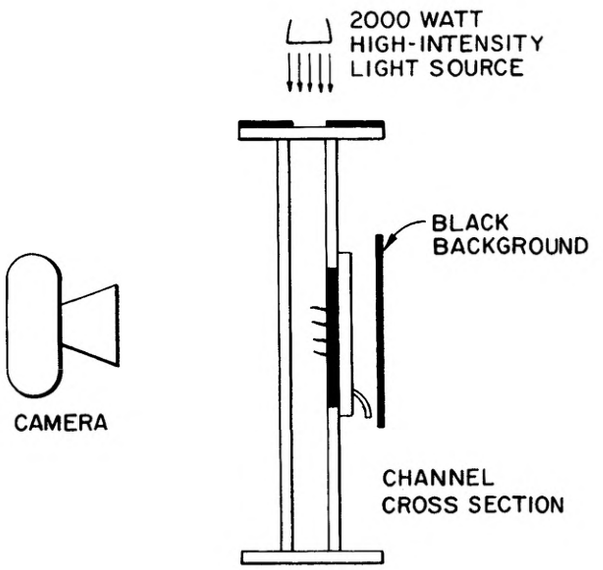

FIGURE 1a. LIGHTING AND VIEWING ARRANGEMENT FOR STREAK-SPACING MOVIES USING THE FLUORESCENT DYE TECHNIQUE

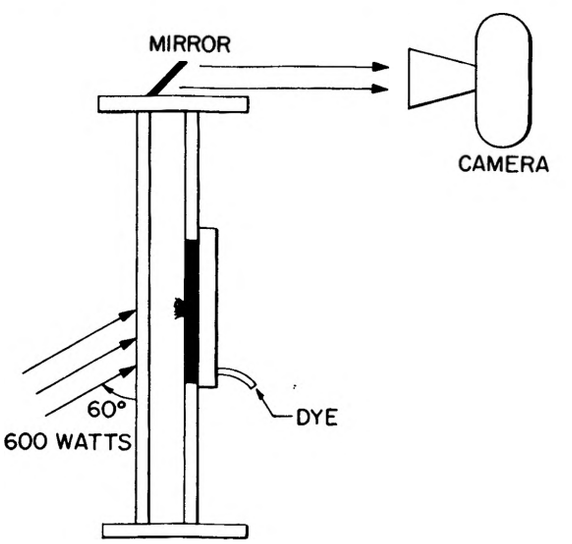

FIGURE 1b. LIGHTING AND VIEWING ARRANGEMENT FOR BURSTING RATE MOVIES

upon a minimum spanwise spacing between streaks, but streaks were always counted at an approximate non-dimensional distance downstream of the dye slot of $x^+ = 1000$. Oldaker (1974) showed that the non-dimensional streak spacing $\lambda^+ = \bar{\lambda}\, u_\tau/\nu$ is independent of x^+ in this region.

Considerable care was taken to ensure that the data reduction process was consistent and statistically reproducible. In most cases the films were simultaneously and independently reduced by five to eight observers. The number of frames counted from each movie varied because, depending upon the flow condition, a single frame would contain from about 3 to 15 streaks. More than 100 but generally less than 300 streaks were counted for each flow condition. The average number of streaks per frame were calculated for each observer and then the mean and standard deviation of these averages were used to determine $\bar{\lambda}$ and the 95% confidence intervals. When replicate reductions were made the final mean was based upon all of the data.

Bursting Rates. Two different schemes or methods were used to make the bursting rate movies and to deduce bursting rates from the top view motion pictures. The essential differences of the two methods are the extent of the field of view in the downstream direction and the criteria for choosing these fields of view. In both methods, the spanwise dye slot length should be less than or equal to $\bar{\lambda}$, so that the probability of one burst obscuring another burst is minimized.

In the traditional method I, the streamwise, the field of view must be large enough in the streamwise direction so that the observer can see bursts from all of the streaks marked at the dye slot. The number of bursts from the entire field of view are counted and the bursting period of a streak is calculated from

$$T_b = d_s/\dot{N}\bar{\lambda} \qquad (4)$$

Conceptually $\dot{N}$ is the number of bursts per unit time from all the streaks marked at the dye slot. To make sure that all the bursts were observed, filming was done over several 128 mm segments downstream of the dye slot. This procedure was repeated so that the entire length of the potential viewing area downstream of the dye slot, 0.6 m was analyzed for drag-reducing flows. Only one segment was necessary in water flows. Film records were made at equal flow conditions for $d_s \approx \bar{\lambda}$, and $d_s \approx \bar{\lambda}/9$. The films were viewed in reverse motion because it was easier to identify the events by watching dye return to the wall.

In method II, the streamwise field of view is small but the location must be chosen so as to ensure that all the marked events that occur within the field of view are marked by the dye. Then discrete realizations of T_b are obtained from a temporal record of the bursting events within this small field of view. Since the bursting event occurs over a period of time rather than at a specific instant, a time T_1 was recorded when the measurement region was first disturbed by an ejection from the burst returning to the wall. (Again the movies were viewed in reverse.) A time T_2 was recorded when the last ejection of the burst disturbed the measurement region. An average time $(T_1 + T_2)/2$ was used as a reference time to compare with the previous burst's reference time. The difference between these two reference times is by definition, an individual bursting period and the average period is simply the arithmetic average of the individual periods. The measurement region had a streamwise length of 12 mm. Bursts that originated within this region as well as bursts from an upstream location that passed over the measurement region within $0 < y^+ \lesssim 30$ were included in the temporal record.

RESULTS

Streak Spacing

One of the important differences between the spanwise spacing of the low-speed streaks in drag-reducing flows as compared to flows of water (solvent) is shown in Fig. 2. The non-dimensional spacing is shown as a function of the ratio of the flow rate within the viscous sublayer and the flow rate of dye injected through the wall slot for 3 levels of drag reduction. Notice that the scale for M is non-linear and inverse. Therefore, approximate y_d^+ locations for the distance normal to the wall which was marked initially by dyed fluid are also shown in Figure 2. These estimates were

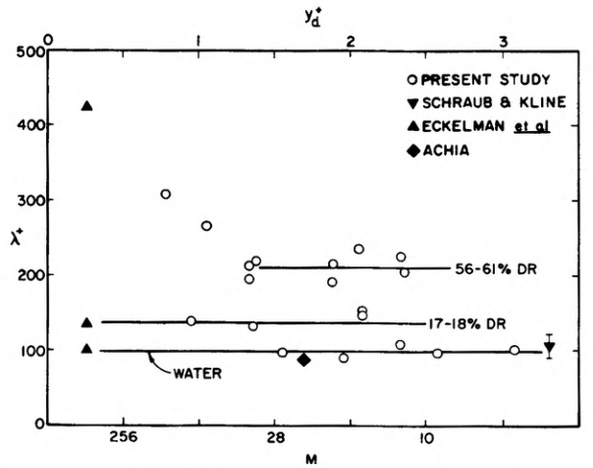

FIGURE 2. VARIATION OF STREAK SPACING WITH DYE FLOW RATE AND DISTANCE FROM THE WALL

made from continuity considerations by assuming that the dye stays next to the wall in a laminar sheet. This is obviously not the case but the estimates are useful as a guide to indicate the relative thickness of the marked region which must increase as the dye flow rate increases.

There is clearly a marked difference between the water flows and the flows with drag reduction in the range of 56-61%. For water flows the non-dimensional streak spacing is not a function of dye flow rate over the range $7 < M < 27$ and λ^+ has a characteristic value of 100 in the range $0.5 < y_d^+ < 4$. The water point of Schraub and Kline (1965) is from a hydrogen bubble wire located at $y^+ = 3.3$. The points extrapolated from the results of Eckelman et al. (1972) are at essentially $y^+ \leq 0.5$, because the high Schmidt number mass transfer boundary layer formed by the electrochemical technique is within these limits. The drag-reducing flows near the 18% level also showed no change in streak spacing as the dye flow rate was varied. In contrast, the non-dimensional streak spacing for flows with drag reductions of 56-61% increased from values of λ^+ near 200 to values above 300 as the dye flow rate was decreased.

Since there was a concern that this increase in λ^+ could be due to an insufficient concentration of dye in the viscous sublayer, two experiments were conducted where the only difference was the concentration of the dye. In both cases, M was set equal to 18 and the polymer solution, flow, lighting and filming conditions were identical. However in one case the dye was made up at its regular concentration while in the second case the dye was diluted by a factor of 5. For the regular dye concentration $N_s = 5.19 \pm 0.63$ and for the diluted dye $N_s = 5.86 \pm 0.80$. There is only a 10% probability that these two average number of streaks per frame are statistically different at the 95% confidence level. This is strikingly different from the comparison that can be made between the experiments at the regular dye concentration for M = 18 and M = 108. In this case there is a 99.9% probability (95% confidence level) that the M = 108 average of 3.63 ± 0.66 is statistically different from 5.19 ± 0.63. Thus it is reasonable to conclude that the non-dimensional spacing of the streaks is a function of y^+ within the sublayer of flows at the higher levels of drag reduction while λ^+ does not vary within the viscous sublayer of either solvent flows or flow at small values of drag reduction.

This variation of λ^+ with y^+ at the higher levels of drag reduction explains the difference between the previously reported results of Eckelman et al. (1972) and Donohue et al. (1972). Their data are compared to data from the present study in Figure 3. Here the only data shown from the present study are from experiments where $5 < M < 15$ and consequently the flows were marked by dye out to y^+ values of at least 2 or more. The present results which include data from experiments with two concentrations of

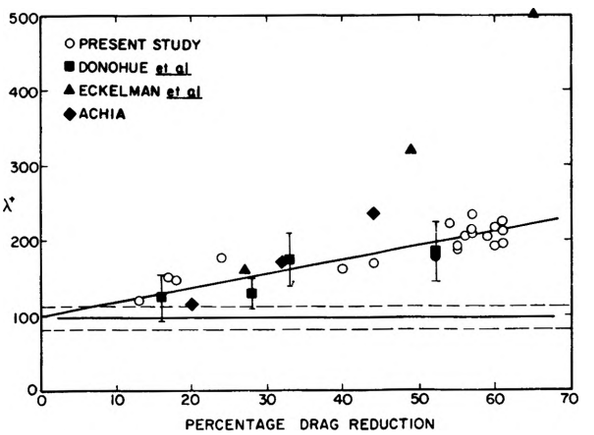

FIGURE 3. STREAK SPACING VARIATION WITH DRAG REDUCTION

Separan AP 273 (polyacrylamide), one concentration of Magnifloc 837-A (polyacrylamide) and one concentration of Polyox WSR-301 (polyethylene oxide) agree with the Polyox-FRA data of Donohue et al. (1972). It is believed that in all of these experiments the streaks were marked and counted in a comparable range of y^+. The Separan AP 30 data of Achia & Thompson (1974) is in good agreement except for the point at 44% drag-reduction. However, for this data point the flow rate of the slot-injected enhancer were slightly less than 3% of the sublayer flow rate and therefore the flow structure was marked closer to the wall. The data of Eckelman et al. (1972), which represent the flow structure for $y^+ < 0.5$, are also in good agreement for values of drag reduction less than about 35%.

Bursting Rates

As might be expected the amount of dye flow rate through the injection slot also affects the bursting rate measurements. These effects are shown in Figures 4 and 5 which are streamwise histograms of the number of ejections per unit time and per unit area, $\dot{N}_E''$. These histograms were generated by dividing the total field of view into increments of 25.4 mm and then by counting the ejections of individual dye filaments from each of these small increments over a period of time. Throughout this study the distinction made by Offen and Kline (1974) between a burst and an ejection has been used.

Physically $\dot{N}_E''$ should be a constant in these flows. The problem of course is that it is not possible to first mark and then to see all of the bursting events with a slot injection. Therefore as shown in Figure 4 the maximum value of the histograms moves upstream as M decreases. This result is consistent with the previous hypothesis that the higher dye flow rates (smaller values of M) mark a thicker portion of the viscous sublayer because the streaks do not eject fluid until after they thicken and lift away from the wall. However, notice that the maximum magnitude in Figures 4a and 4b is essentially constant at $\dot{N}_E'' = 3.5$. This is an important result because it suggests that all of the bursting events were marked by the dye in these maximum magnitude regions. In fact Smith (1975) also conducted experiments at M = 6, 12 and 150 for the drag-reducing flow shown in Figures 4a and 4b. At M = 6 the dye was jetting away from the wall as it came out of the slot. At M = 150 ejections were not seen for $x^+ <$ 1800 and within the observation distance $\dot{N}_E''$ rose only to about 2. However, the histogram for M = 12

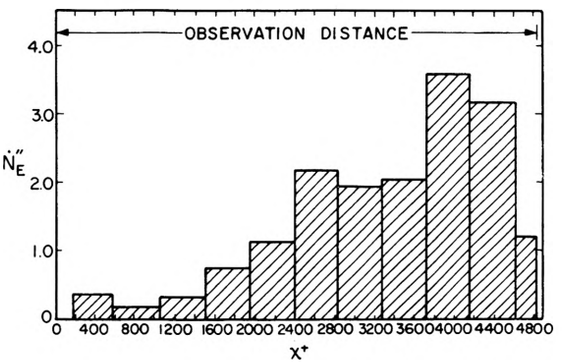

FIGURE 4a. HISTOGRAM OF EJECTION RATE PER UNIT AREA FOR D_R = 17.25%, M = 29, u_τ = 0.0158 m/s

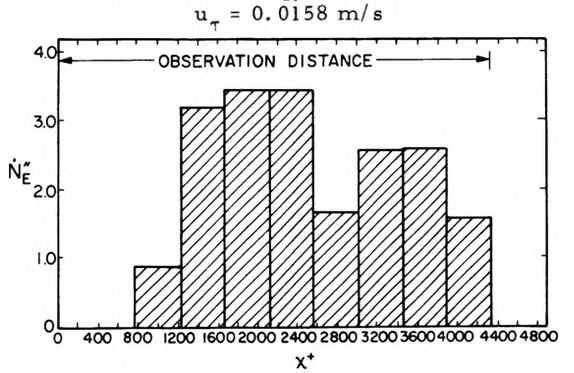

FIGURE 4b. HISTOGRAM OF EJECTION RATE PER UNIT AREA FOR D_R = 17.25%, M = 9, u_τ = 0.0158 m/s

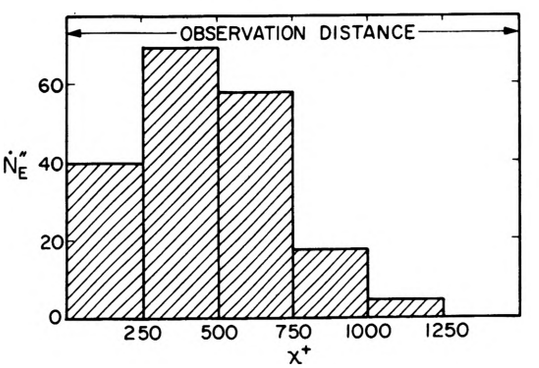

FIGURE 5. HISTOGRAM OF EJECTION RATE PER UNIT AREA FOR A WATER FLOW, u_τ = 0.0173 m/s, M = 9

was consistent with the results shown here.

By comparing Figures 4 and 5 it is apparent that a relatively small streamwise observation distance is needed for counting all of the bursting events marked by a slot injection in a water flow. A much larger distance is required in a drag-reducing flow and the required observation distance in a drag-reducing flow is very sensitive to the dye flow rate. A similar sensitivity to M was not seen in water flows (see Smith 1975). Consequently, it is apparent that to properly execute measurement method I the observation distance must be relatively large and, practically, the dye flow rate should be adjusted so that $M \approx 10$. For measurement method II, the observations must be made in the maximum magnitude region and its location, which is dependent upon the value of M, must be determined prior to the construction of the temporal record of bursting events.

The results from the bursting period measurements are summarized in Tables 1 and 2. In all cases $M \approx 10$ and therefore a value of $\overline{\lambda}$ was extrapolated from the average line drawn through the streak-spacing results for $y_d^+ \geq 2$ shown in Figure 3. Several things are obvious from the tabulated results. By comparing the results from water experiments at the same flow condition but with different dye slot lengths, it is apparent that bursting periods from method I and Equation 4 are not equal. The reason for this discrepancy is that the bursting events apparently have a spanwise size of about $\overline{\lambda}$ and therefore Equation 4 is not valid when $d_s < \overline{\lambda}$. As shown in Table 1 the values of 1/N are reasonably equivalent. Similarly with method II, different dye slot widths yield equivalent values of T_B. Since the size of the bursting events is of order $\overline{\lambda}$, the method I results with $d_s \approx \overline{\lambda}$ are better estimates of T_b than the results with a $d_s \approx \overline{\lambda}/9$.

It is also apparent that the bursting periods given by method II are about a factor of 5 to 6 larger than the periods given by Equation 4 when $d_s \approx \overline{\lambda}$. This point will be discussed further later in this section.

TABLE 1. SUMMARY OF BURSTING RESULTS (METHOD I)

Type of polymer	Concentration of polymer (ppm)	D_R (%)	u_τ (m/s)	$d_s/\overline{\lambda}$	$d_s/(\dot{N}\overline{\lambda})$ (s)	$1/\dot{N}$ (s)
none	0	0	0.0173	1.20	0.26	0.22
none	0	0	0.0173	0.10	0.034	0.35
none	0	0	0.0208	0.98	0.19	0.18
none	0	0	0.0205	0.11	0.031	0.27
Calgon TRO 323	100	33	0.0234	0.96	0.22	0.20
Separan AP 273	50	40	0.0166	1.19	0.53	0.45
Separan AP 273	50	41	0.0168	0.14	0.13	0.61

TABLE 2. SUMMARY OF BURSTING MEASUREMENTS FROM A SMALL REGION (METHOD II)

Type of polymer	Concentration of polymer (ppm)	D_R (%)	u_τ (m/s)	$d_s/\overline{\lambda}$	T_b (s)	T_d (s)
none	0	0	0.0173	1.20	1.01 ± 0.25	0.93 ± 0.32
none	0	0	0.0173	0.10	1.03 ± 0.18	0.410 ± 0.074
none	0	0	0.0205	0.11	0.694 ± 0.075	0.350 ± 0.066
none	0	0	0.0208	0.98	0.638 ± 0.101	0.397 ± 0.109
Calgon TRO 323	100	33	0.0234	0.96	1.31 ± 0.331	1.14 ± 0.483
Calgon TRO 323	100	17	0.0208	0.16	0.973 ± 0.153	0.53 ± 0.16
Separan AP 273	50	40	0.0166	1.19	1.32 ± 0.31	0.78 ± 0.31
Separan AP 273	50	41	0.0168	0.14	1.26 ± 0.14	0.93 ± 0.22

The bursting period results are compared in various non-dimensional formats with the results of other investigators in Figures 6, 7, and 8. Figures 6 and 7 show the results in Newtonian flows while Figure 8 summarizes the drag-reducing results. In Figures 6 and 7 the time between bursts has been normalized with "inner" variables while an "outer" variable normalization has been used in Figures 7 and 8. The momentum thickness, θ, and the displacement thickness, δ^*, were calculated from their definitions using the channel flow velocity profiles predicted by the eddy diffusivity scheme developed by Tiederman and Reischman (1976). For the channel flows the centerline velocity U_o was used in place of the free stream velocity in a boundary layer and the channel half-width or tube radius, D/2, was assumed to be equivalent to the boundary layer thickness, δ.

The water results shown in Figures 6 and 7 indicate that the present results using method I with $d_s \approx \bar{\lambda}$ agree with previous reported values of T_b. The scatter in the data is high but it is also clear that the method I measurements of Donohue et al. (1972) and Achia and Thompson (1974) show an increase in the normalized bursting periods when the Reynolds number is below 600. The reason for this increase is not clear but there are at least two possibilities. For example, fully developed, turbulent, internal flow may be simply inherently different from turbulent boundary layers due to the absence of an interaction between an outer, wake, portion of the shear layer and and the near-wall region in the internal flow. The other possibility is that there is a Reynolds number dependence for the bursting process at low Reynolds number because the spectrum of turbulent motions may be too narrow to yield the high Reynolds number behavior. In any case it is clear that further research is needed to completely understand the correlation of bursting periods.

Method II yields a lower bursting rate and hence the values of T_b are high compared to the previous hot-wire and visual measurements. It is believed that method II is fundamentally a different measurement because its upstream "coherence" length is probably significantly

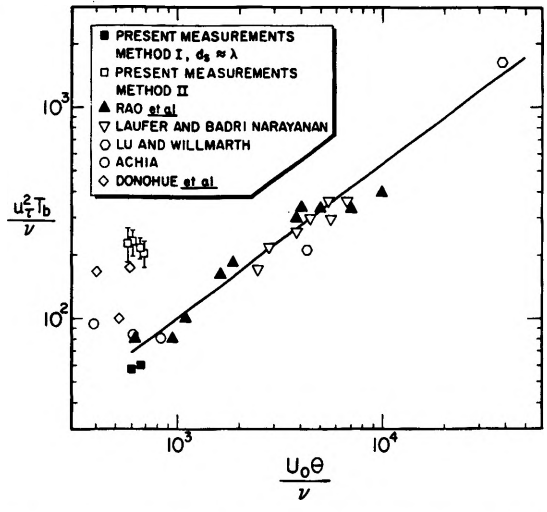

FIGURE 6. BURSTING PERIODS IN NEWTONIAN FLOWS NORMALIZED WITH INNER VARIABLES

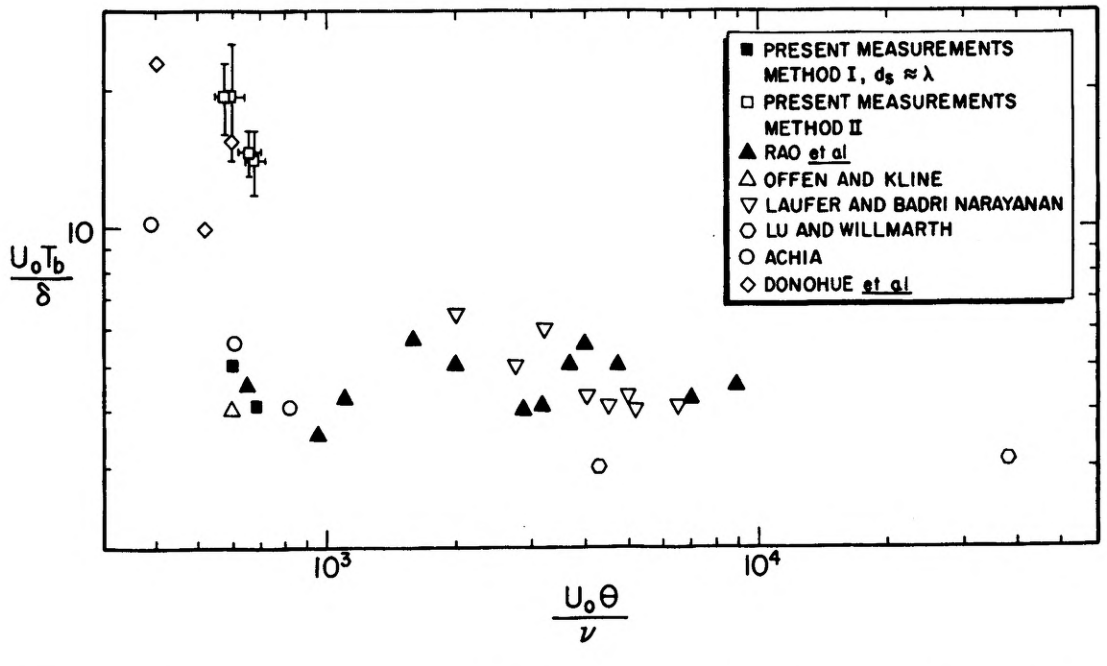

FIGURE 7. BURSTING PERIODS IN NEWTONIAN FLOWS NORMALIZED WITH OUTER VARIABLES

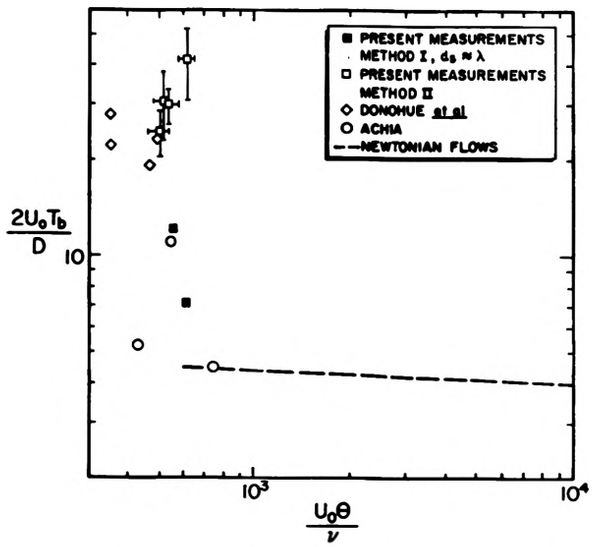

FIGURE 8. BURSTING PERIODS IN DRAG-REDUCING FLOWS

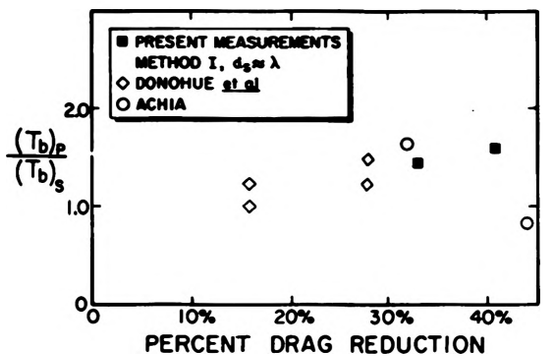

FIGURE 9. RATIO OF BURSTING PERIODS IN DRAG-REDUCING AND WATER FLOWS AT EQUAL SHEAR VELOCITY

shorter than that of either a hot wire at $y^+ = 15$ or a perpendicular hydrogen bubble wire. That is, method II appears to yield a more local result than the other visual or hot-wire methods for measuring T_b. Consequently, the method II results may be particularly applicable to surface renewal models. For example, the non-dimensional bursting periods $(T_b/\nu)^{1/2}u_\tau$ measured in water flows with method II are between 14 and 15. These values are the same order of magnitude as the data summarized by Meek (1972).

The results for drag reducing flows shown in Figure 8 also clearly indicate that the normalized bursting periods increase as the Reynolds number decreases in this low Reynolds number range. The agreement with the data of Donohue et al. was not totally unexpected. Even though their field of view was short, they used a relatively high dye flow rate. Again the method II results are high.

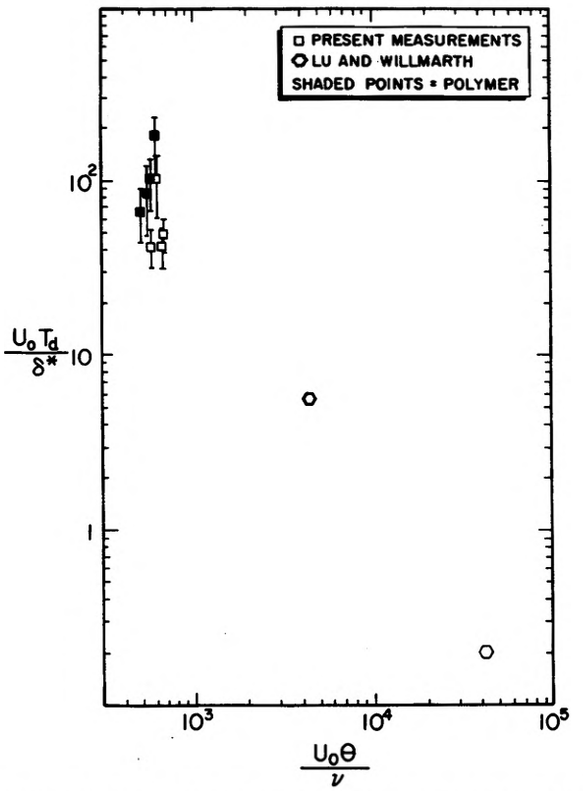

FIGURE 10. BURSTING DURATION IN NEWTONIAN AND DRAG-REDUCING FLOWS

The ratios of the bursting period of a streak in a drag reducing flow compared to the bursting period in a water flow at the same wall shear stress are shown in Figure 9. Except for one of Achia's points, all of the data indicate that the low-speed streaks are slightly more stable in the drag-reducing flow. This coupled with the increased spacing of the streaks yields a significant decrease in the spatially averaged bursting rate. Although the data is not plotted here, a similar comparison using method II bursting periods yields a similar result.

The temporal duration of a burst may also be determined from the method II measurements. The average durations of bursts, T_d, are shown in Table 2 and in Figure 10. Notice that the normalized durations agree with the trend indicated by Lu and Willmarth's (1973) data. There does not appear to be a significant difference between the average duration of a burst in a drag-reducing flow compared to a similar water flow.

CONCLUSIONS

This study shows that none of the structural features of the Newtonian near-wall region are totally

suppressed during drag reduction. However, some are altered. Not only does the average spanwise spacing of the low-speed streaks increase as drag reduction increases, but the average spacing also increases as y^+ decreases. This result does not appear to depend upon either the concentration or the type of polymer used. Combinations which yield equal amounts of drag reduction have the same average non-dimensional spanwise spacing.

The spanwise extent of a bursting event is on the order of $\bar{\lambda}$; and in a drag-reducing flow, the downstream location of bursting events marked by a slot injection is very sensitive to the dye flow rate. However, when these facts are considered it is possible to accurately measure bursting periods with dye from a slot injection. The bursting measurements indicate that the streaks in a drag-reducing flow are somewhat more stable than those in a water flow at the same wall shear stress. This combined with the increased spacing yields a significant decrease in the spatially averaged bursting rate.

ACKNOWLEDGEMENTS

This work was supported by the National Science Foundation, Grant GK-40609 and by the Office of Engineering Research, Oklahoma State University.

NOMENCLATURE

D	width of the channel
D_R	percentage drag reduction, see Equation 1
d_s	spanwise length of the dye slot in use
M	ratio of flow rate in the undisturbed viscous sublayer over the dye slot to the flow rate of dye through the slot, see Equation 2
$\dot{N}$	number of bursts per unit time from all of the streaks marked at the dye slot
$\dot{N}''_E$	number of ejections per unit area and per unit time
N_s	average number of streaks for a given experimental condition
$\dot{Q}_d$	flow rate of the dye
T_1	time when the measurement region in method II was first disturbed by burst "i"
T_2	time when the measurement region in method II ceased being disturbed by burst "i"
T_b	average period of a burst; for method I this is is given by Equation 4; for method II

$$T_b = \frac{1}{N} \sum_{i=1}^{N} [T_r(i+1) - T_r(i)]$$

T_d	average duration of a burst,

$$T_d = \frac{1}{N} \sum_{i=1}^{N} [T_2(i) - T_1(i)]$$

T_r	reference time for burst "i", $T_r = (T_1 + T_2)/2$
U_o	centerline velocity in the channel
u_τ	shear velocity, $u_\tau = (\tau_w/\rho)^{1/2}$
x	distance downstream of dye slot
x^+	$x^+ = (xu_\tau)/\nu$
y	distance normal to the wall
y^+	$y^+ = (yu_\tau)/\nu$
y_d^+	estimate of distance normal to the wall initially marked by dye
P_p	pressure drop in a drag reducing flow
P_s	pressure drop in a solvent flow
δ^*	displacement thickness
θ	momentum thickness
$\bar{\lambda}$	average spanwise spacing of streaks, see Equation 3
λ^+	$\lambda^+ = \bar{\lambda}u_\tau/\nu$
ν	kinematic viscosity
ρ	density
τ_w	wall shear stress

REFERENCES

1. Achia, B. U., 1975, "Structure of Pipe Wall Turbulence in Newtonian and Drag-Reducing Flow: A Hologram-Interferometric Study", Ph.D. Thesis, The University of British Columbia.

2. Achia, B. U., and Thompson, D. W., 1974, "Laser Holographic Measurement of Wall-Turbulence Structures in Drag-Reducing Pipe Flow", presented at BHRA International Conference on Drag Reduction, Cambridge, England.

3. Donohue, G. L., Tiederman, W. G., and Reischman, M. M., 1972, "Flow Visualization of the Near-Wall Region in a Drag-Reducing Channel Flow", J. of Fluid Mech., 56, p. 559.

4. Eckelman, L. D., Fortuna, G., and Hanratty, T. J., 1972, "Drag Reduction and the Wave Length of Flow-Oriented Wall Eddies", Nature, 236, p. 94.

5. Laufer, J. and Badri Narayanan, M. A., 1971, "Mean Period of the Turbulence Production Mechanisms in a Boundary Layer", Phys. Fluids, 14, p. 182.

6. Lu, S. S. and Willmarth, W. W., 1973, "Measurement of the Mean Period Between Bursts", Phys. Fluids, 16, p. 2012.

7. Lu, S. S. and Willmarth, W. W., 1973, "Measurements of the Structure of the Reynolds Stress in a Turbulent Boundary Layer", J. of Fluid Mech., 60, p. 481.

8. Meek, R. L., 1972, "Mean Period of Fluctuations Near the Wall in Turbulent Flows", AIChE Journal, 18, p. 854.

9. Offen, G. R., and Kline, S. J., 1974, "Combined Dye-Streak and Hydrogen-Bubble Visual Observations of a Turbulent Boundary Layer", J. of Fluid Mech., 62, p. 223.

10. Oldaker, D. K., 1974, "An Experimental Investigation of the Near-Wall Flow Structure During Drag Reduction", M.S. Thesis, Oklahoma State University.

11. Rao, K. N., Narasimha, R., and Badri Narayanan, M. A., 1971, "The Bursting Phenomenon in a Turbulent Boundary Layer", J. of Fluid Mech., 48, p. 339.

12. Reischman, M. M. and Tiederman, W. G., 1975, "Laser Doppler Anemometer Measurements in Drag-Reducing Channel Flows", J. of Fluid Mech., 70, p. 369.

13. Runstadler, P. W., Kline, S. J., and Reynolds, W. C., 1963, "An Experimental Investigation of the Flow Structure of the Turbulent Boundary Layer", Report MD-8, Stanford University.

14. Schraub, F. A. and Kline, S. J., 1965, "A Study of the Turbulent Boundary Layer With and Without Pressure Gradients", Report MD-12, Stanford University.

15. Smith, A. J., 1975, "An Investigation of the Bursting Events in Drag-Reducing Turbulent Channel Flows", M.S. Thesis, Oklahoma State University.

16. Tiederman, W. G. and Reischman, M. M., 1976, "Calculation of Velocity Profiles in Drag-Reducing Flows", Trans. ASME, J. of Fluids Engrg., 98,